A Composite Study of Comma Clouds and their Association with Severe Weather over the Great Plains

FREDERICK H. CARR AND JAMES P. MILLARD[1]

School of Meteorology, University of Oklahoma, Norman, OK 73019

(Manuscript received 1 June 1984, in final form 14 November 1984)

ABSTRACT

Sixty-eight comma-cloud systems over the Great Plains during two spring seasons were examined using satellite imagery and rawinsonde data. Composite soundings were produced for each of ten distinct parts of the comma cloud in order to describe quantitatively the atmospheric structure associated with wave cyclones that produced 585 severe weather events. Composite sectionals and soundings document the different kinematic and thermodynamic environment of each part of the comma-cloud system. Relative-wind, isentropic analyses show air flow relative to the storm and provide additional evidence that the clear region intruding northward east of the cyclone center is an area of strong ascent of dry air with a previous history of subsidence. Stability computations from the mean soundings suggest that the most likely location for severe weather is near the central part of the comma tail, in agreement with the tabulated severe weather reports.

A case study from 21–22 March 1981 is conducted to investigate the generation of a secondary line of convection which formed in the center of a dry intrusion after the main area of convection passed to the east. This "dry-slot convection" is hypothesized to occur if the upper cloud edge of the comma tail moves ahead of the associated surface boundary during the day, leaving a region of moist boundary-layer air exposed to solar heating. With rising motion, adiabatic cooling and drying aloft, and increasing warming and moisture convergence near the surface, a rapid destabilization can occur, resulting in development of secondary lines of convection vigorous enough to produce severe weather.

1. Introduction

Since the early 1960s, satellite imagery has provided the operational meteorologist with an invaluable tool for observing the evolution of tropospheric cloud patterns. The key to the usefulness of this tool lies in our ability to relate correctly the imagery to common meteorological phenomena such as fronts, jets, vorticity centers and areas of precipitation. The objective of this paper is to contribute to our quantitative understanding of atmospheric structure and behavior associated with the commonly observed comma-cloud systems over the Great Plains states.

From the beginning, studies have shown that the cloud patterns associated with midlatitude cyclones evolve through a sequence of identifiable stages that are remarkably in agreement with the classical wave cyclone models. Studies by Boucher and Newcomb (1962), Leese (1962), Widger (1964) and others correlated the cloud features with various stages of cyclone development and concluded that advective processes are as important as the vertical motion distribution in creating the observed patterns. Barr *et al.* (1966) investigated this quantitatively with a 10-level quasi-geostrophic model and found that the cloud pattern resembles the computed rising motions during the early stages of the cyclone but horizontal motions become more important as the storm matures. Carlson (1980) studied the airflow of a developing wave cyclone in a relative-wind, isentropic system to determine more precisely how the familiar comma-cloud pattern evolves. He found that the northern and eastern part of the pattern evolve from the southerly "warm conveyor belt" (Browning, 1971; Harrold, 1973) while the westward extension which forms part of the comma head originates from east of the low via a "cold conveyor belt." More studies such as this are needed to further our knowledge of trajectories and moisture transport in wave cyclones.

In addition to the specific papers mentioned above, a number of survey reports have been compiled by Anderson *et al.* (1972), Miller and McGinley (1978), Weldon (1979) and others. They have elucidated many of the qualitative relationships between the satellite imagery and the kinematic features seen on surface and upper-air charts. The time now seems right to begin to document the *quantitative* structure of the atmosphere associated with certain cloud systems. The system we have chosen to investigate is the large-scale comma pattern associated with baroclinic waves as they traverse the Great Plains. To

[1] Current affiliation: USAFETAC, Scott Air Force Base, Illinois, 62225.

increase the reliability of the results, we have constructed a composite from over 60 such systems. The composite approach has proved extremely useful in previous studies (e.g., Williams and Gray, 1973; Mullen, 1979) over the oceans and should prove equally valuable here.

The purpose of this paper is two-fold. In the first part, the composite kinematic and thermodynamic structure associated with the comma cloud will be presented on pressure and relative-wind, isentropic surfaces. Mean soundings, stability profiles and preferred severe weather locations will also be discussed. In the second half, a case study will be examined to illustrate a phenomenon we shall call "dry-slot convection." This event refers to the generation of thunderstorms and squall lines in the northern part of the dry intrusion, behind the main lines of convective precipitation associated with the warm and cold fronts. Dry-slot convection will be shown to be a result of a predictable sequence of destabilizing mechanisms occurring in that region.

2. Compositing technique

The study was limited to comma-cloud systems which formed or traversed over the Great Plains during the 1980 and 1981 spring seasons (March–June). In order to be selected, the comma cloud had to be associated with the large-scale circulation of a wave cyclone (see Fig. 1). The cloud system could be just beginning to organize into a comma shape or be representative of an occluded cyclone, with dry air spiraling around the center. Figure 1 is typical of a cyclone which is just beginning to occlude and represents a medium stage in the life cycle of the cases chosen for this study. Thirty-five distinct systems were found during the eight month period. Since many of these systems maintained a comma shape during two or more rawinsonde times, a total of 68 time periods is included in the composite.

Based on GOES visual and infrared imagery, each system was divided into ten zones, five (A, B, C, D, E) which sectioned the cloudy region and five (1, 2, 3, 4, 5) which partitioned the dry intrusion. The selection of ten zones was a compromise between the spacing needed to resolve important parts of the system and the average distance between rawinsonde stations. Figure 1 shows a mature comma cloud pattern seen in infrared satellite imagery for 10 May 1981. The zones defined above are marked on the relevant parts of the system as an example of the subjective compositing method. Zone A represents the "comma head" while zone B is the northernmost part of the comma cloud. Zones C, D, and E represent north-to-south sections of the "comma tail," which is usually associated with a surface cold front. Dry

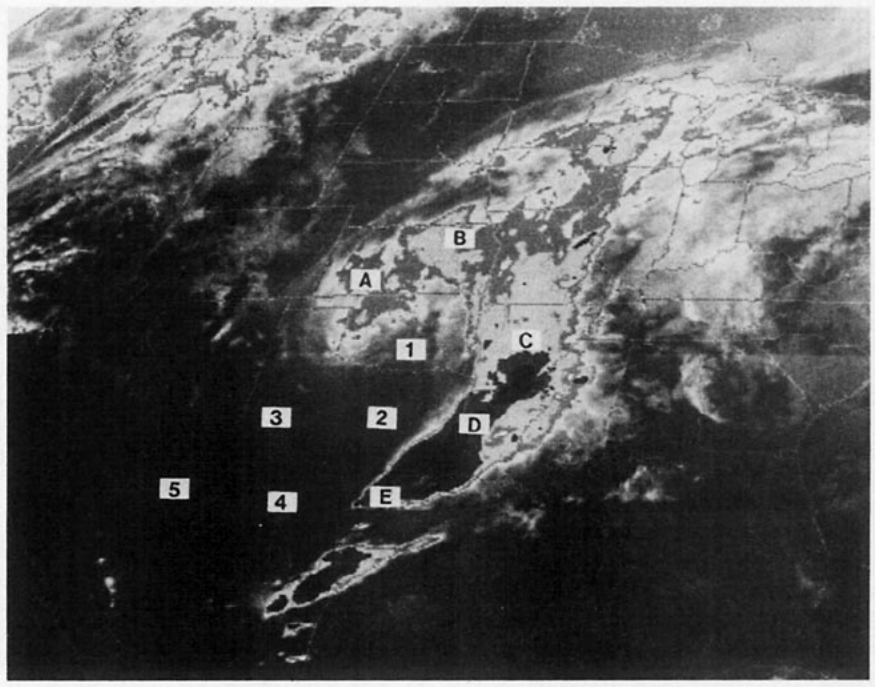

FIG. 1. Example of a comma cloud seen in infrared imagery with the five cloudy zones labeled A–E and the five clear zones labeled 1–5. The rawinsonde stations selected for each zone are: A—Dodge City, KS; B—Topeka, KS; C—Little Rock, AR; D—Longview, TX; E—Victoria, TX; 1—Oklahoma City, OK; 2—Stephenville, TX; 3—Midland, TX; 4—Del Rio, TX; 5—Chihuahua, Mexico.

air entering the cyclone system from the southwest forms the feature known as the "dry tongue" (we shall use dry "tongue" or "slot" or "intrusion" or "surge" interchangeably). Zone 1 is included only if the dry tongue has penetrated north of the center of the comma head to the west.

Once the zones were identified from satellite imagery nearest the synoptic rawinsonde release time, the sounding closest to the center of each zone was selected for the composite. It is important to note that only soundings *within* a zone were used, not just the nearest ones. Thus each zone has a different number of soundings included in the composite. Figure 1 represents a relatively rare case in which rawinsonde stations were found for all zones (see figure caption for the station names). Figure 2 shows the idealized, schematic comma-cloud pattern which will be used to display the sectional results. The number of soundings included in each zone are shown. Zone 1 has the fewest since a cyclone must be fully developed before the dry slot begins to intrude around the comma head, but the sample size should be large enough to construct a representative composite.

Standard and significant-level rawinsonde wind, temperature and moisture data were interpolated from 1000 to 100 mb in 25 mb increments and then averaged to form a composite sounding for each zone. Since the maximum dew point depression reported is 30°C, this value was used for all "dry" reports. Because the actual depression may have been much greater, the effect of this assumption is to underestimate the depressions shown in zones 2–5. Note that since the wind averaging was done using the u and v components, the magnitude of the composite vector is *less* than the average wind speed in each zone.

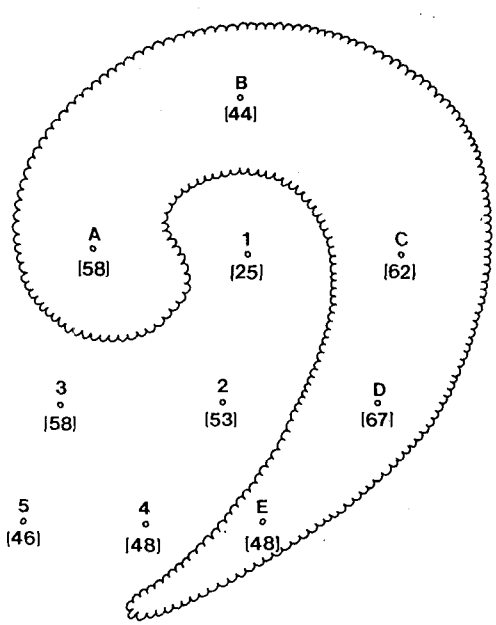

FIG. 2. Schematic diagram of a comma cloud showing the location of the ten zones. The number of rawinsonde reports used in each zone is in brackets.

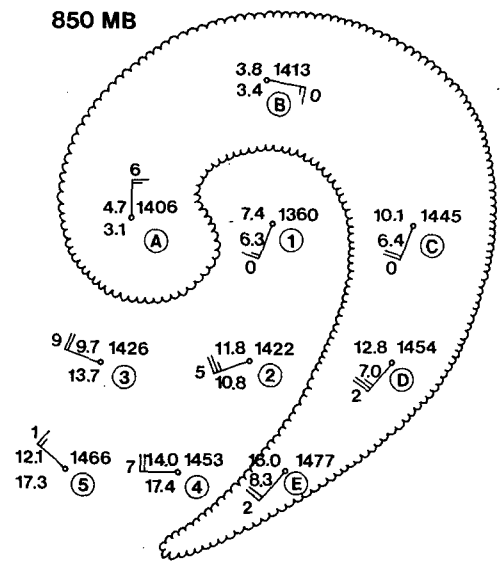

FIG. 3. Composite upper-air data at 850 mb. Temperature and dew point depression in °C are to the left of the station circle. Upper right value is height in m. Full wind barb: 5 m s^{-1}, half barb: 2.5 m s^{-1}, flag: 25 m s^{-1}. The ten's digit of the wind direction is plotted at the end of each wind staff.

3. Composite results

a. Isobaric sectionals

Composite sectionals were constructed for all standard upper-air levels above 1000 mb. Figure 3 displays the results at 850 mb. The wind field defines a closed vortex halfway between zones A and 1. The winds are essentially aligned along the comma-cloud pattern, although the 850 mb warm front shows up clearly between zone B to the north and zones 1 and C to the south. Zones D and E in the comma tail are both warmer and more moist than the zones immediately to their west, indicating a strong gradient of equivalent potential temperature θ_e across the cloud edge. Zones A and B to the north have smaller dew point depressions than those in the comma tail, though, owing to the greater frequency of stratiform versus convective clouds and precipitation there. Finally, the moisture in zone 1 is surprisingly high, reflecting the fact that the leading edge of the dry air in the middle troposphere (see Figs. 4 and 5) is downstream of the low-level moisture boundary. It should be noted, though, that the standard deviation of the dew point depressions was largest in this zone (7.3°C), partly because of the smaller sample and the fact that the moist layer was occasionally below 850 mb.

Figures 4 and 5 show 700 mb and 500 mb com-

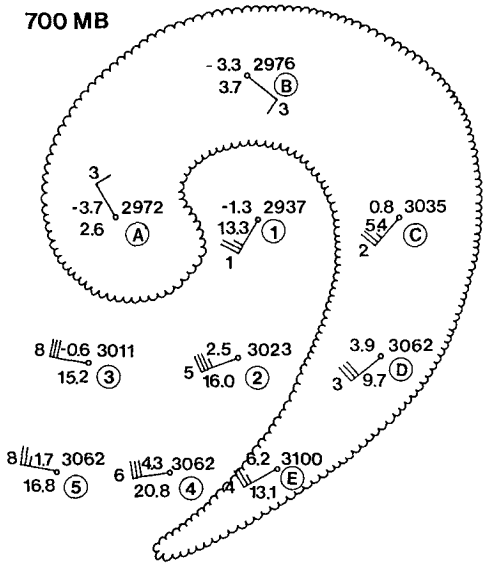

FIG. 4. As in Fig. 3 except for 700 mb.

posites. The wind field near the comma head provides evidence that the composite low is tilting to the west-northwest toward the coldest temperatures, which are in zone A at all levels between (but not including) 850 and 300 mb. The circulation is closed up to 400 mb and becomes an open wave above there. The wind speed maximum is located in zone 2 in all the mid- and upper-tropospheric composites. This suggests deceleration (and perhaps convergence) at the western boundary of the comma tail, which agrees with the observations of Weldon (1979).

The western edge of the comma tail also continues to identify a strong θ_e gradient at 700 and 500 mb. The dry tongue signature is most pronounced at 500 mb where zones 1 to 5 all have dew point depressions at least 11°C larger than climatology (Crutcher and Meserve, 1970). Note that since zone 1 dries out rapidly above 850 mb and is nearly as cold at upper levels as zone A, the northern part of the dry slot represents an area where potential instability increases with time during its formative stage.

One interesting aspect of Figs. 3–5 is that, despite the averaging and coarse resolution, evidence exists for some of the mesoscale structure of the dry tongue as discussed by, e.g., Kreitzberg and Brown (1970), Harrold (1973), and summarized by Browning and Monk (1982). If a surface boundary were to be drawn on, e.g., Fig. 3, it would start from the surface low between zone 1 and the eastern edge of the comma head, curve eastward and then southward, and may cross the comma tail at its southern tip. This boundary, if located in the southern Great Plains, is often a dry line (Schaefer, 1974). The western edge of the midtropospheric cloud boundary in zones C and D (Figs. 4 and 5) represents the "upper cold front" which is the leading edge of the "overrunning dry air" in the Browning and Monk (1982) split-front model. This low θ_e air represents a source of potential instability as it overrides the moist air below and partially explains the deep convection often observed on the western edge of the comma tail.

The 300 mb sectional (Fig. 6) is representative of an upper-tropospheric composite. The vorticity center is now in the region between zones A and 3. The lowest height value remains in zone 1 because of bias in the sample; i.e., zone 1 exists over a significant region only in well-developed cyclones while, by our

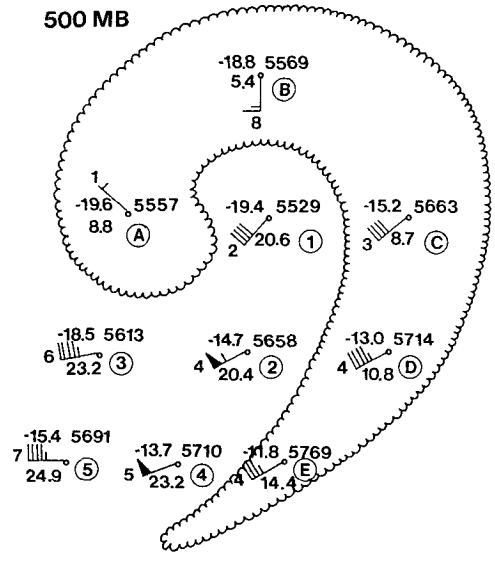

FIG. 5. As in Fig. 3 except for 500 mb.

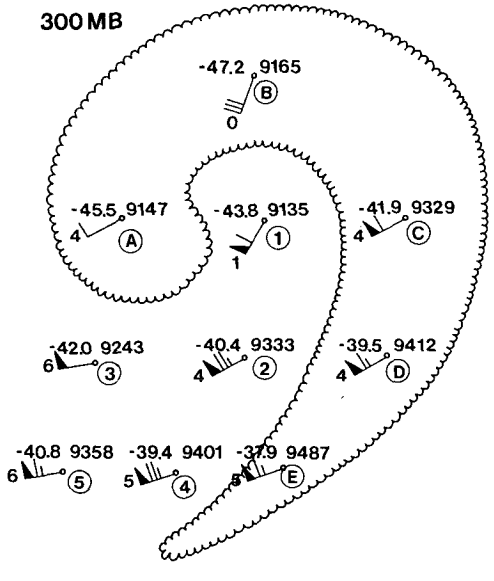

FIG. 6. As in Fig. 3 except for 300 mb.

definition, all comma systems have "heads" and "tails" (recall the number of available soundings indicated in Fig. 2). In contrast to lower levels, all the winds now blow across the comma pattern, creating the large cirrus shield seen east and northeast of a wave cyclone. There is evidence of two speed maxima at 200 mb (not shown). One extends across the southern part of the comma cloud while the other is associated with the dry tongue and extends from zone 5 to zone C. This is consistent with the upper-level difluence frequently observed downstream from the trough line. Figure 6 shows that this difluence exists between zones B and E, and indicates, to the extent that severe weather is associated with this configuration as suggested by McNulty (1978) and others, that severe weather events would be concentrated in zones C and D (see Table 2).

The composite wind speed maximum is 43 m s^{-1} at 200 mb in zones 4 and E (not shown). Zone B, which contains the temperature minimum in the upper troposphere, is the warmest zone at 100 mb, the lower stratosphere. All of the composite winds at 100 mb blow from 260°.

b. *Isentropic, relative-wind composites*

As discussed by Green *et al.* (1966), Carlson (1980) and others, the assumption that a system translates in a steady-state manner allows one to subtract the translation vector from the observed winds to obtain winds relative to the system. If we also assume that the large-scale flow is adiabatic and we plot the relative winds on isentropic surfaces, the resulting streamlines can also be considered as *trajectories* relative to the system. This procedure is now applied to the composite comma-cloud data to obtain a quantitative picture of airflow with respect to what is seen on the satellite imagery. Since the composite comma system is unsaturated in all zones, no attempt was made to construct wet-bulb potential temperature surfaces in cloudy regions. For individual cyclones, this procedure is recommended, as shown by Carlson (1980).

The average translation vector of the composite wave cyclone was computed from the average of the mean phase velocity at three levels: surface, 700 mb and 500 mb. This mean translation vector was found to be from 255° at 9 m s^{-1} and was subtracted from all the observed winds after they were interpolated to the isentropic surfaces. The fact that all parts of the comma system do not translate at the same speed is a weakness of this technique. Three relative-wind, isentropic surfaces are constructed with the lower troposphere being represented by the 297 K surface. A 10°C increment in the vertical is used, with the 307 K surface representing the lower-to-middle troposphere and the 317 K surface displaying conditions in the middle-to-upper troposphere.

An estimate of the vertical motion component of the flow (with respect to pressure) along an isentropic surface can be made from

$$\omega = \frac{dp}{dt} = \left.\frac{\partial p}{\partial t}\right|_\theta + \mathbf{V}_\theta \cdot \nabla_\theta p + \frac{d\theta}{dt}\frac{\partial p}{\partial \theta}, \qquad (1)$$

where the θ subscript indicates that the quantity is evaluated on an isentropic surface and the other symbols have their usual meteorological meanings. Assuming steady-state, adiabatic flow and converting to natural coordinates, we can write (1) as

$$\omega \approx V_r \left.\frac{\partial p}{\partial s}\right|_\theta, \qquad (2)$$

where s is the coordinate along the trajectory and V_r is the relative wind speed ($=|\mathbf{V}_\theta - \mathbf{V}_c|$, where $\mathbf{V}_c$ is the mean phase velocity). To calculate the derivative in (2), we first computed the average latitude and longitude of the center of each zone using the location of all the selected rawin stations. Assuming the composite data to be valid for the center of each zone, the mean distances between the zones are known. A natural coordinate system is then constructed in the center of each zone to evaluate $\partial p/\partial s|_\theta$, with Δs taken to be 200 km. Owing to all of the assumptions involved, vertical velocity values from (2) are not expected to be precise but should be in general qualitative agreement with the typical vertical motion values associated with wave cyclones.

Figures 7, 8 and 9 display the composite relative-wind, isentropic results at 297, 307 and 317 K, respectively. Vertical velocity, pressure and dew point depressions are plotted in each zone. The dashed lines are isobars analyzed every 50 mb and they portray the baroclinic environment in which the comma cloud exists. It is clear from all three levels that the thermal pattern lags the wind field such that significant warm and cold advection occurs on the eastern and western parts respectively of the comma system. In fact, under the adiabatic, steady-state assumption, use of Poisson's equation with (2) shows that temperature advection is the only cause of vertical motion; i.e.,

$$\omega \approx \frac{c_p p}{RT} V_r \left.\frac{\partial T}{\partial s}\right|_\theta. \qquad (3)$$

In other words, the vorticity advection contribution has been eliminated by the phase velocity correction required by the relative-wind procedure.

In Fig. 7, streamlines are also drawn to highlight the kinematic structure at low levels. The relative circulation center near 800 mb is located on the eastern edge of the comma head. The streamlines suggest that a deformation zone at 900 mb is located between zones 2, 4 and E. Its position is consistent

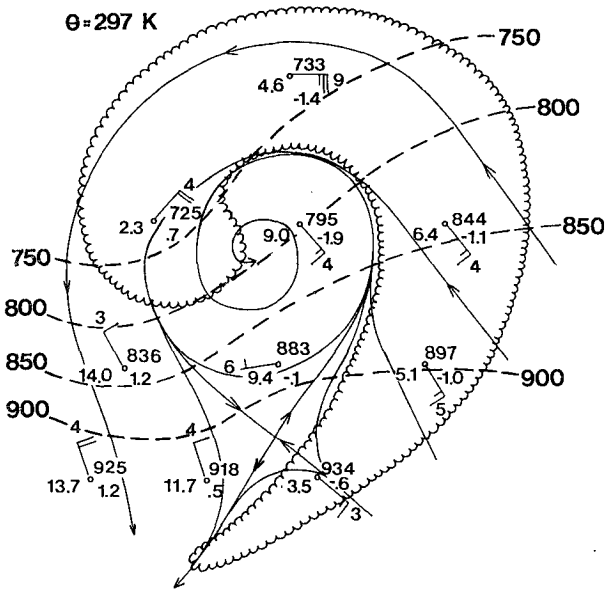

FIG. 7. 297 K relative-wind isentropic surface. Value to upper right of station circle is pressure in mb; to lower right is vertical motion in μb s^{-1}; to lower left is dew point depression in °C. Wind convention is the same as in Fig. 3. Dashed lines are isobars drawn every 50 mb; solid lines are streamlines.

with a surface cold front (associated with the comma tail) which is sloping northwestward with height. Since the angle between the apparent axis of dilatation and the isobars (equivalent to isotherms if on a pressure surface) is less than 45°, frontogenesis is occurring in this region (Petterssen, 1936). The vertical motions are all upward in the cloudy regions except in the comma head which is undergoing weak subsidence. This is consistent with Carlson (1980), whose

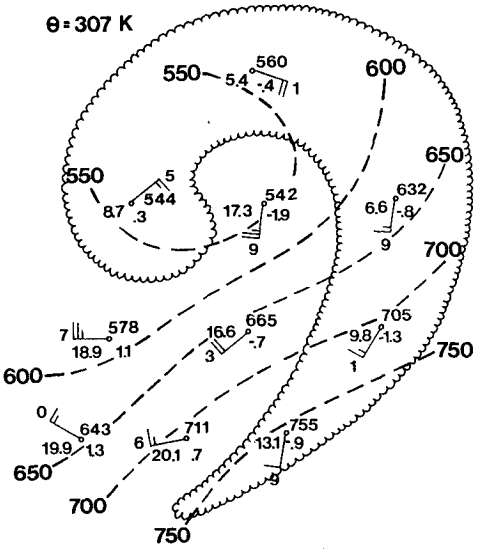

FIG. 8. As in Fig. 7 except for 307 K surface and streamlines are not drawn.

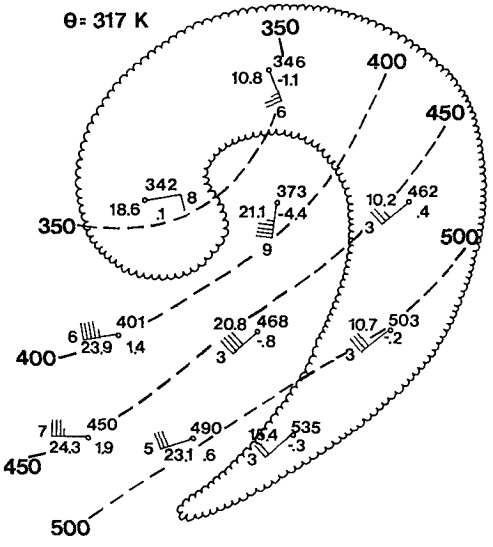

FIG. 9. As in Fig. 8 except for 317 K surface.

trajectories also showed that this part of the comma cloud evolves from the advection of cool, low-level moist air from the east. Note that the air at upper levels above the comma head (Figs. 8 and 9) becomes much drier than in zones B and C, in agreement with infrared imagery which indicates warmer and, hence, lower cloud tops in this region (e.g., see Fig. 1).

On all three θ-surfaces, the strongest upward vertical velocities are in zone 1, the clear, northern end of the dry tongue. This is partly due to the zone 1 bias discussed in the previous section but should not invalidate the previous statement. This distribution confirms the observation by Leese (1962) that the dry slot is a region of *rising motion* as dry air with a previous history of subsidence surges northeastward around the midtropospheric circulation center. Leese's observation is further supported by the dry air and sinking motion calculated in zones 3, 4 and 5, the southwestern part of the comma system. The strong rising motion in zone 1 also implies significant adiabatic cooling and destabilization in the middle-to-upper troposphere.

Note that the weaker upward velocities in the cloudy regions could be substantially enhanced if saturated ascent is considered. The effect of the resulting condensation, of course, is to cause the upward trajectories to become steeper and rise toward lower pressures and larger potential temperatures. This additional lift can be computed from

$$\frac{\theta}{c_p T} H \frac{\partial p}{\partial \theta},$$

where H is the diabatic heating rate due to condensation. For example, a 10 mm per day rainfall rate (equivalent to 5°C d^{-1} temperature increase through

a 500 mb layer) leads to a 1 $\mu b\ s^{-1}$ increase in upward motion for typical stability values. Since rainfall rates often exceed the above value even in nonconvective regions, it is clear that mean upward velocities in zones B to E are significantly larger than the computed values.

Figures 8 and 9 show that the relative circulation center remains closed off above 350 mb and slopes westward with height. The southern part of the comma head is the location of the mid- and upper-tropospheric relative circulation center. Since all of the composited cyclones are embedded in a basic westerly current, the easterly flow in zones A and B at middle and upper levels indicates the presence of a relative deformation zone north of the storm. Weldon (1979) has discussed the importance of this feature in determining the actual evolution of the cloud pattern revealed by satellite imagery. The winds at 307 and 317 K continue to imply speed convergence along the western edge of the comma tail and also suggest that the western cloud boundary is an asymptote of confluence at midlevels, at least along the southern part. As mentioned in the last section, this is consistent with the upper cold front in the Browning and Monk (1982) model, and can also be interpreted as the "limiting streamline of the warm conveyor belt" (Carlson, 1980).

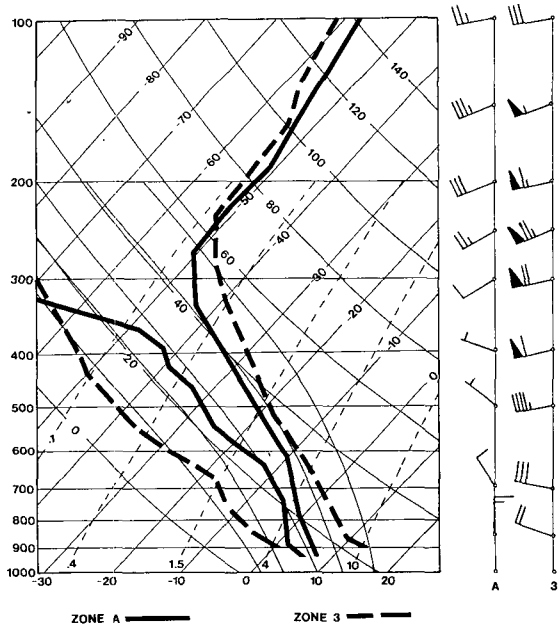

FIG. 10. Composite skew$T$ – log$p$ diagram for zones A (solid lines) and 3 (dashed lines). Temperatures are shown to 100 mb and dew point temperatures shown to 300 mb. Horizontal solid lines are pressure in mb; temperature lines in °C run from lower left to upper right; dry adiabats (°C) from upper left to lower right. Five moist adiabats are shown in the vicinity of the soundings and the thin dashed lines are saturation mixing ratios (g kg^{-1}). Winds are plotted to right with a full barb: 5 m s^{-1}, half barb: 2.5 m s^{-1}, and flag: 25 m s^{-1}.

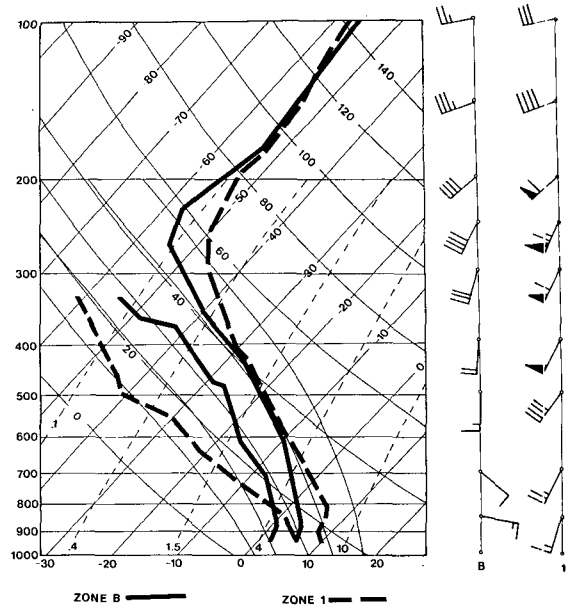

FIG. 11. As in Fig. 10 except for zones B and 1.

The pressure difference between two isentropic surfaces is inversely proportional to static stability. Inspection of the differences between the surfaces portrayed in Figs. 7–9 reveals that low-level stability is greatest in zone B while zone 5, well behind the dry line, has the lowest stability. At upper levels, zones 1 and C are most stable while 4 and E are least stable.

c. *Composite soundings*

A few of the composite soundings are shown in Figs. 10 and 11. Zones A and 3 are plotted together in Fig. 10 to illustrate the differences between the air in the comma head and that south of it. Zone A is much cooler and is nearly saturated up to 650 mb. The northerly winds at low levels back with height to west-southwesterly flow in the upper troposphere, indicating both the cold advection on the west side of the surface low and the tilt of the cyclone from the eastern edge of the comma head to the southern edge. The source of air for zone 3 is completely different than zone A, as there are westerly winds at all levels, resulting in a warmer and much drier sounding.

The composite soundings of zones B and 1 are contrasted in Fig. 11. Zone B has the highest mean 1000–500 mb relative humidity (71%) of all zones, and, as mentioned before, the greatest low-level static stability. The relative winds which bring air into this region are from the east up to 500 mb (see Fig. 8), while the veering seen in the observed winds in Fig. 11 indicates strong warm advection. In short, this is a classic example of a mean sounding 100–200 km north of a warm front. South of the warm front in

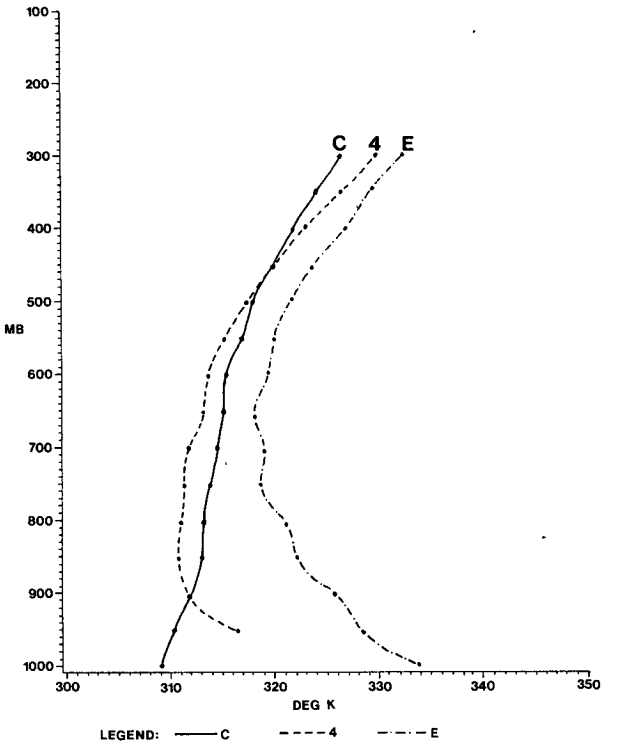

FIG. 12. Composite equivalent potential temperature (K) for zones C, E and 4.

the northern part of the dry tongue (zone 1), the winds show little directional shear but strong speed shear, as this region lies just on the cyclonic shear side of the upper-tropospheric isotach maximum.

There is an elevated stable layer in the low levels of the zone 1 composite sounding. When the individual soundings are examined, nearly all show a pronounced low-level inversion at 1200 GMT and a less-marked (or nonexistent) one at 0000 GMT. The fact that the thickness of the inversion is different for each case also contributes to the poor definition of the inversion in the composite sounding. An attempt was made to composite the soundings with respect to the inversion location. For example, in zone 1, the average inversion base and top were 860 mb and 830 mb, respectively. The mean static stability

$$\sigma = -\frac{RT}{p\theta}\frac{\partial\theta}{\partial p}$$

in the inversion was 6.0×10^{-6} m^2 s^{-2} Pa^{-2} and only 1.7×10^{-6} m^2 s^{-2} Pa^{-2} in the 100 mb layer above it. Because of the arbitrary nature of adjusting the lapse rates above and below the stable layer in order to create a sounding composited with respect to the inversion which yields the same geopotential height values, no figures of these results are shown. The key points concerning zone 1 are that the sounding is potentially unstable in the morning, this instability is usually released by 0000 GMT via dry or moist convective overturning, and this convection could be severe due to the strong winds aloft and the delaying effect of the inversion.

The contrasts between zones C, E and 4 can best be seen by comparing equivalent potential temperature profiles (Fig. 12). Zone E has a tropical character, reflecting the Gulf of Mexico moisture which is usually present in this zone. Potential instability is greatest in this zone and exists up to 650 mb. A surface dry line usually exists between E and zone 4 to the west, especially at 0000 GMT, and accounts for the much lower θ_e values in the zone 4 sounding. There is a sharp decrease of θ_e in the boundary layer of zone 4, indicating the dry adiabatic lapse rate commonly found behind dry lines. Above 850 mb, θ_e increases with height. Zone C, on the other hand, shows $-\partial\theta_e/\partial p > 0$ at all levels, despite being a zone of much convective activity (see Table 1). The main reason for this is the large diurnal range of boundary layer θ_e in zone C. In the morning, this zone is near

TABLE 1. Values of the SWEAT Index at 0000 and 1200 GMT for each zone computed from the composite data.

	Zone									
	1	2	3	4	5	A	B	C	D	E
					1200 GMT soundings					
Shear part	25	—	—	—	—	—	—	74	55	42
Dynamic part	70	107	95	87	77	35	46	75	102	84
Low-level moisture	17	—	—	—	—	11	—	20	53	76
Stability part	—	—	—	—	—	—	—	—	—	—
SWEAT Index	112	107	95	87	77	46	46	169	210	202
					0000 GMT soundings					
Shear part	105	—	—	—	—	—	—	109	97	78
Dynamic part	76	91	87	84	80	28	59	78	95	81
Low-level moisture	4	37	—	—	—	31	17	77	95	96
Stability part	—	—	—	—	—	—	—	—	—	—
SWEAT Index	185	128	87	84	80	59	76	264	287	245

or north of a surface warm front, while clearly south of the front at 850 mb (recall Fig. 3). The cool surface temperatures and associated inversion lead to large morning static stability values. In most of the 0000 GMT soundings in this zone, the surface is significantly warmer and more moist, with strong potential instability up to 700 mb.

The development of potential instability during the day in each of the zones was monitored by computing lifted indices and Miller's (1972) "SWEAT Index" separately from the 1200 and 0000 GMT composite soundings. The results for the SWEAT Index, which is defined in the Appendix, are presented in Table 1. It should be noted that since mean soundings are used, none of the values exceed Miller's threshold value of 300 for severe thunderstorms; nevertheless, the diurnal differences are quite revealing. Zone D has the largest SWEAT Index at both times, as it is the region with the best combination of dynamic and thermodynamic forcing. The diurnal change in zone C, as discussed in the previous paragraph, is very large as its 0000 GMT value becomes larger than the zone E value. A significant diurnal increase is also noted for zone 1, which will be elaborated on further in Section 4.

d. Relation to severe weather

Severe weather reports (U.S. Dept. of Commerce, 1980, 1981) were tabulated for each of the dates used in the composite. Severe weather was defined as tornadoes, funnel clouds, hail > 19 mm and surface winds > 26 m s^{-1}. The results, stratified by zone, are presented in Table 2. Eighty percent of all severe weather reports were located in zones C, D and E. Zone D was the most likely region for severe weather and had 47% of all tornadoes. Composite hodographs (not shown) indicated that zone D has speed and directional shears of 20 m s^{-1} and 80° respectively in the 1000–500 mb layer. Closer inspection revealed that most of this activity occurred near the western edge of D, i.e., in association with the advancing cold front or dry line in that region. Zone A had a fair number of funnel and tornado reports, indicating that one should be alert for these "cold air" events in the comma head, especially on its eastern edge (Cooley, 1978). Although not very many severe weather events occurred in zones 1 and 2, convective lines often formed there and would move eastward into zones C or D before any severe activity had developed. This is consistent with the relatively large number of hail reports in zone 1, since large hail is commonly the first severe event in the life cycle of a severe storm (Browning, 1965).

TABLE 2. Number of severe weather events occurring in each zone for the cases included in the composite.

Zone	Hail	Funnels	Tornados	Winds	% by zone
A	19	10	15	9	9
B	2	1	3	2	1
C	47	11	32	47	23
D	70	26	73	49	37
E	52	27	24	13	20
1	23	7	6	6	7
2	7	2	1	1	2
Events	220	84	154	127	585

4. A case study of dry-slot convection

a. Synoptic overview

The composite sectionals and soundings of the previous sections indicated that the northern part of the dry tongue (zone 1) is a location where secondary outbreaks of severe convection could occur. Some of the factors responsible for this appear to be: (i) a moist boundary layer to the west of the upper cloud edge (western boundary of zone C); (ii) midtropospheric dry air, indicating potential instability; and (iii) a frontal boundary at the surface and large-scale upward motion aloft, providing mechanisms for the release of the instability. Browning and Monk (1982), noting that the dry air aloft is often 100 km or more ahead of the surface frontal boundary in this region, also mentioned these factors but indicated that intense convection there is rare in the British Isles. Two aspects of Great Plains cyclones which differ from the British systems are that the region between the surface boundary and the upper cloud edge to the east often has only scattered to broken cloudiness rather than solid low overcast, and that the morning low-level inversion over the Great Plains may be stronger, due to the high-θ air advected from the southwest over the cool, moist air near the surface (Carlson *et al.*, 1980). Thus solar radiation is allowed to heat the surface and the inversion prevents early release of the instability. We observed five instances of convective line development that occurred in zone 1 to the west of the primary areas of convection (zones C and D). We shall call this "dry-slot convection." A particularly clear example of dry-slot convection took place on 21–22 March 1981 and is more closely examined in the following sections.

The large-scale synoptic situation for 1200 GMT 21 March (Fig. 13) shows a closed-off 500 mb low which has progressed eastward over the Rocky Mountains into southern Colorado. The thermal field lags the geopotential field as expected, with a −28°C minimum over the south-central Rockies. Surface cyclogenesis in the lee of the Rockies began on 20 March, producing a 985 mb low (resolved as only a −69 m minimum in the NMC 1000 mb analysis shown in Fig. 13) over southwest Kansas by 1200 GMT on the 21st. Most of the precipitation at this

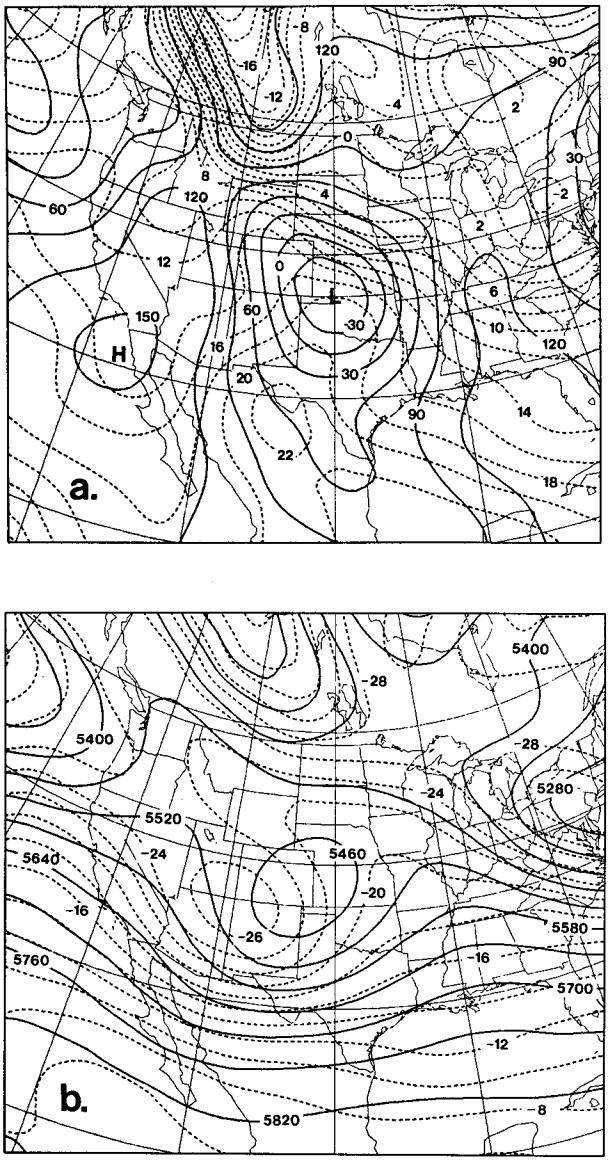

FIG. 13. Height and temperature analyses for 1200 GMT 21 March 1981. Solid lines are contours in m and dashed lines are isotherms in °C. (a) 1000 mb surface, (b) 500 mb surface.

time was confined to the region extending from northeast to northwest of the surface low.

During the ensuing 12 hours, the surface low propagated southeastward across Oklahoma and slowly filled to −23 m (993 mb from surface data) by 0000 GMT 22 March (Fig. 14a). A large area of precipitation broke out during the day from eastern Texas and Louisiana northward through Arkansas and Missouri where it became part of the older precipitation band extending westward to Colorado. Figure 15 is a radar chart valid at 1735 GMT 21 March which is about three hours prior to the outbreak of dry-slot convection in northeastern Oklahoma and southeastern Kansas. The comma shape of the precipitation pattern is clearly evident, and includes rain and thundershowers associated with the comma head over the Texas Panhandle and southwestern Oklahoma. Note the lack of precipitation over eastern Oklahoma and nearly all of Kansas where the dry tongue has been drawn into the storm circulation.

The upper-air structure that existed just after the new convection was initiated is shown in Fig. 14b. The 500 mb low has filled somewhat and is located over central Oklahoma. The most significant change in the midtroposphere is that the temperature field is now nearly in phase with the height field, with the coldest air just south of the 500 mb low. Thus we

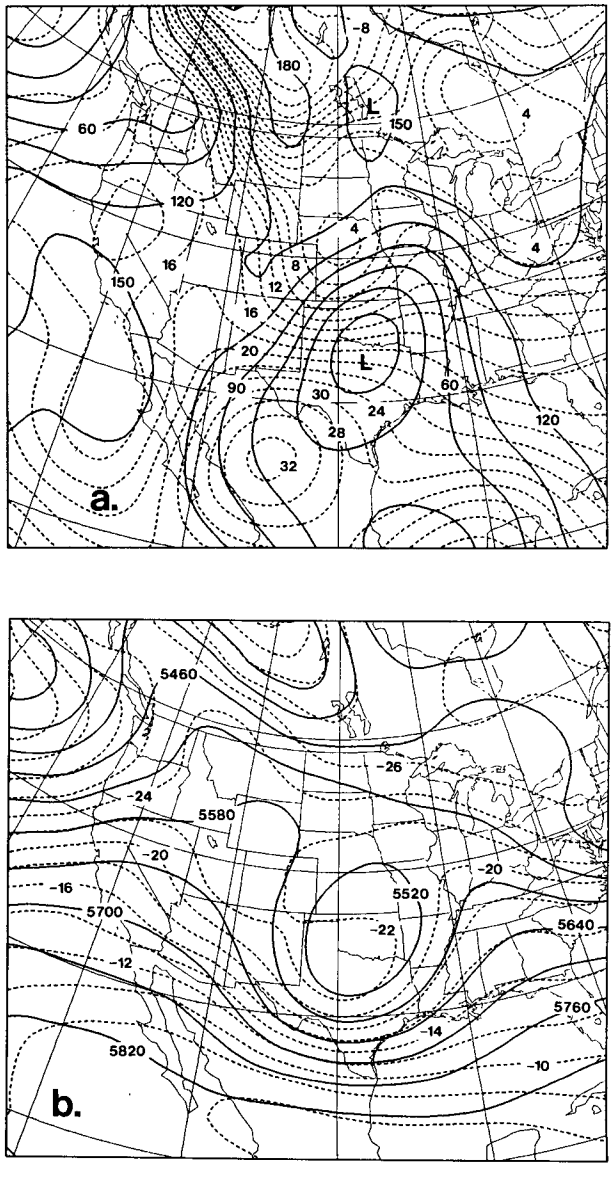

FIG. 14. As in Fig. 13 except for 0000 GMT 22 March 1981.

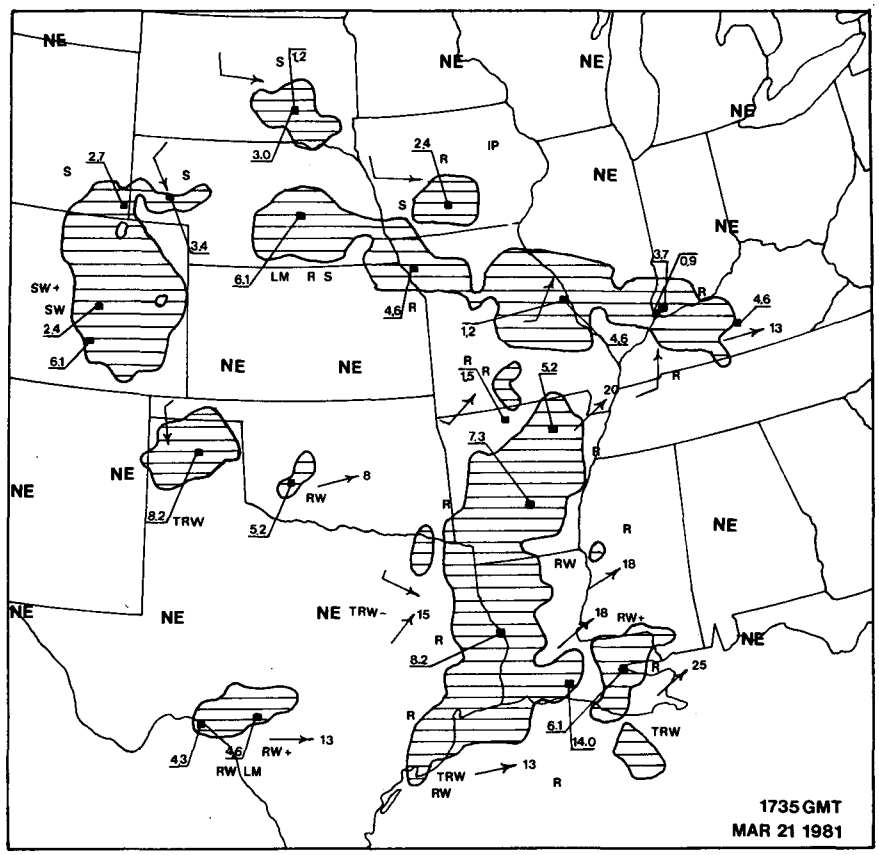

FIG. 15. National Weather Service radar composite for 1735 GMT 31 March 1981. Hatched areas represent precipitation echos; contours are in echo intensities 1, 3 and 5. Echo heights are given in km; system movement is indicated by pennant (full barb: 10 m s^{-1}, half barb: 5 m s^{-1}); cell movement is shown by arrows in m s^{-1}.

observe 2–4°C cooling in eastern Oklahoma even before the trough axis passes over this region. Since this is in the dry intrusion, this result is consistent with the adiabatic cooling implied by the composite vertical motion fields (Figs. 8 and 9).

b. Satellite view

The satellite imagery dramatically illustrates the development of dry-slot convection during the afternoon of 21 March. At 1902 GMT (Fig. 16), the midtropospheric vorticity center is over western Oklahoma. The dry tongue has circulated around the storm and is approaching the Oklahoma Panhandle from the northeast. The sharp cloud edge near the Oklahoma–Arkansas border defines the western edge of zones C and D, separating dry and moist midtropospheric air. Over eastern Oklahoma, a north–south oriented dry line at the surface is located in the middle of the dry slot. Broken stratocumulus clouds east of the dry line indicate the presence of low-level moisture with considerable solar radiation still reaching the surface. Relatively cloud-free air lies between the dry line and the clouds on the eastern edge of the comma head. A large band of blowing dust extends from the New Mexico–Texas border toward Oklahoma.

A larger-scale, infrared view of conditions just before the outbreak of new convection is shown in Fig. 17. This is an excellent portrait of a cyclone just beginning to occlude. Over the eastern part of the dry slot, the infrared imagery reveals warm cloud tops, which supports the view that this is a region of low-level moisture. By 2200 GMT, the dry-slot convection has broken out over eastern Oklahoma and southeastern Kansas (Fig. 18). It is clearly separate from the convection associated with the comma head that is moving into north–central Oklahoma. Visible imagery one-half hour later (Fig. 19) shows a band of convection extending from central Kansas to southeastern Oklahoma. Moist, recently-heated air is fueling the new thunderstorm growth as the line moves eastward.

The 2335 GMT radar chart (Fig. 20) portrays the squall line one hour later. A severe thunderstorm watch has been issued for the southern half of the

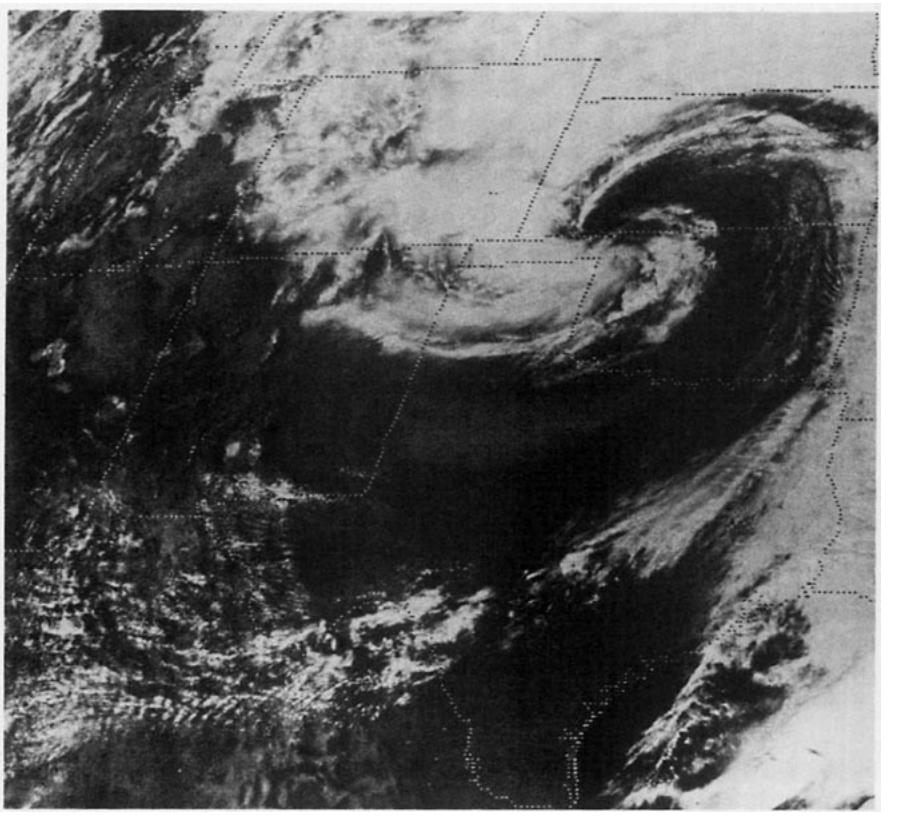

FIG. 16. GOES-E visible imagery for 1902 GMT 21 March 1981.

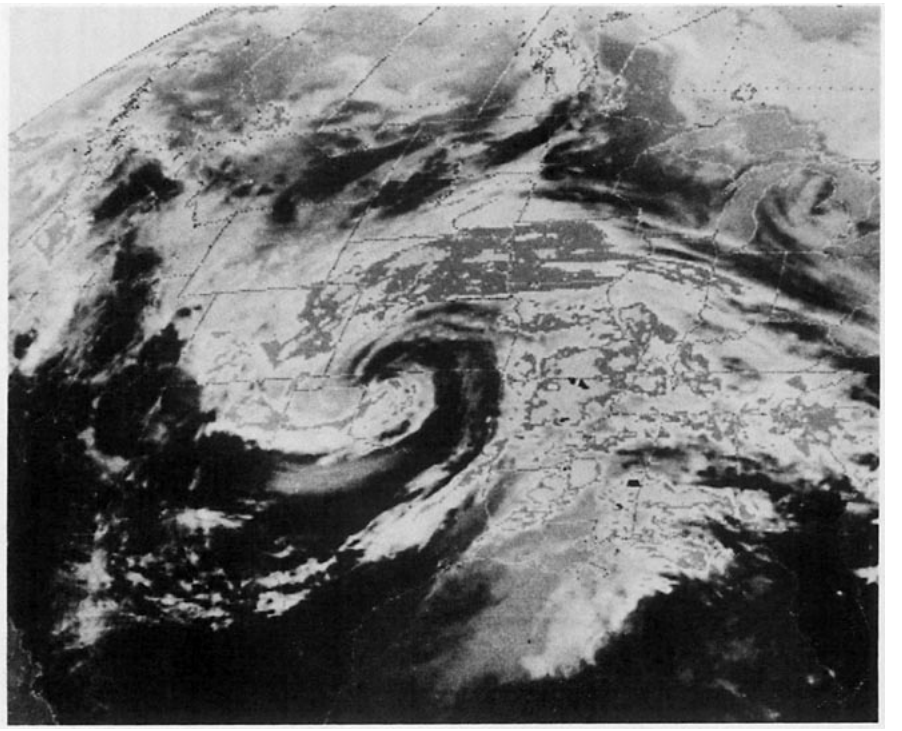

FIG. 17. GOES-E infrared imagery for 2000 GMT 21 March 1981.

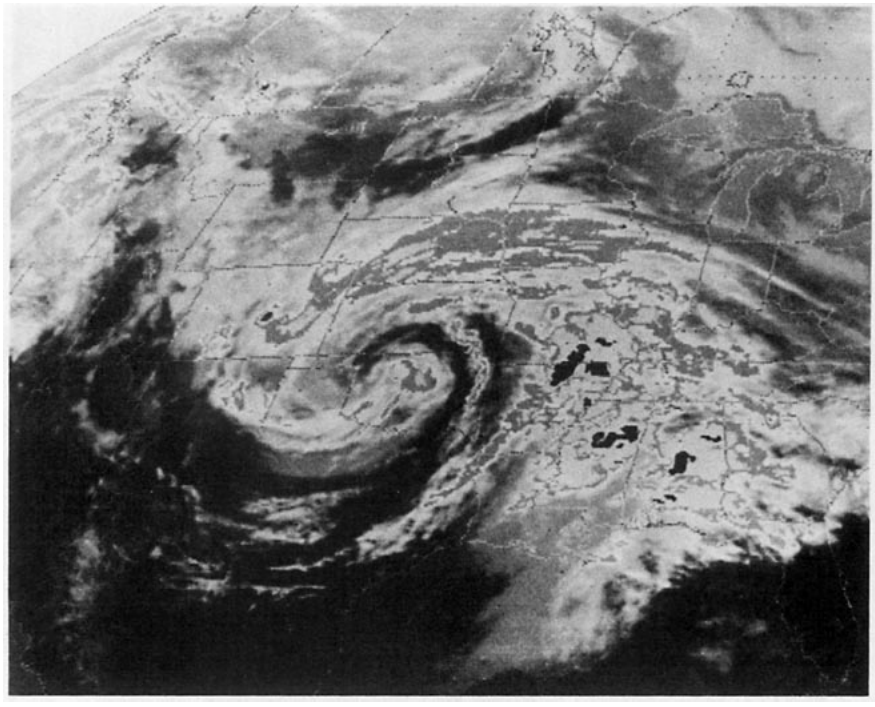

FIG. 18. GOES-E infrared imagery for 2200 GMT 21 March 1981.

line. Maximum cloud tops are 11.9 km at 2335 GMT and grew as high as 13.7 km at 0135 GMT 22 March. This squall line did not generate any tornadoes but produced heavy rain and 19 mm hail as it moved eastward into Arkansas.

c. Surface and sounding features

The satellite sequence indicates that the 2100 GMT surface data would be most instructive. Figure 21 shows a 990 mb low in northwest Oklahoma with a

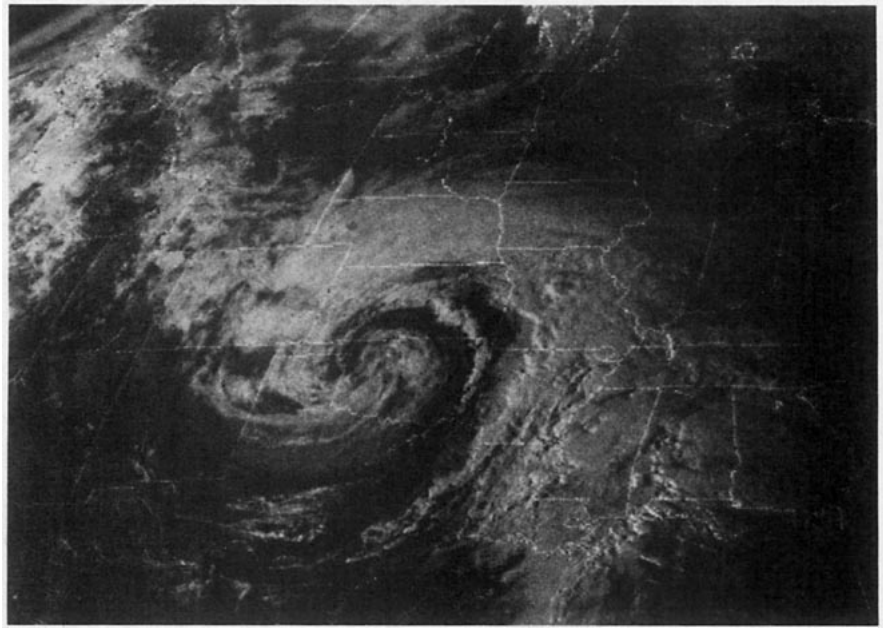

FIG. 19. GOES-E visible imagery for 2230 GMT 21 March 1981.

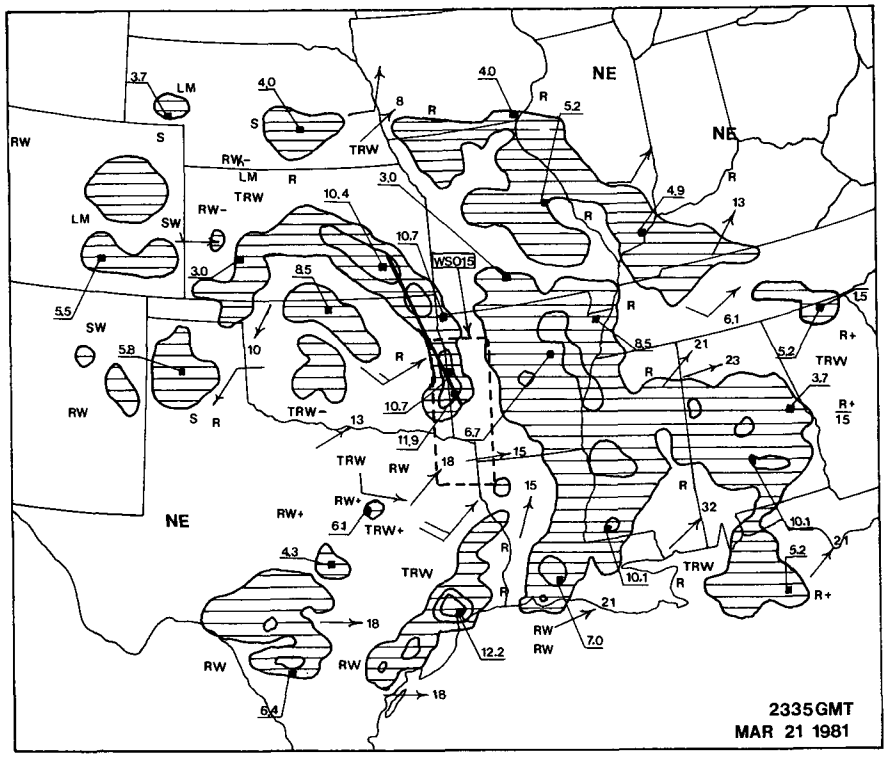

FIG. 20. As in Fig. 15 except for 2335 GMT 21 March 1981.

dry line intruding northward into central Kansas. The dry line extends southward into eastern Oklahoma and Texas and clearly represents an elongated region of moisture convergence. This dry line began as a trough in western Texas and Oklahoma at 1200 GMT but the combination of lower tropospheric subsidence (Fig. 7), downslope warming and greater solar heating at the surface in the drier air all acted to create the warmer, dry air mass behind the wind shift line. A trough associated with the cold front trails southwestward from the low as cooler air surges southward into Texas.

Although no upper-air sounding station exists in the region where the dry-slot convection originated, the squall line was approaching Monettt (UMN) in southwestern Missouri at 0000 GMT 22 March. Figure 22 contains both the morning (1200 GMT) sounding when UMN was between zones B and C and the evening (zone 1) sounding. The temperature profile changed significantly at only two levels (hence the 0000 GMT temperature is not plotted): the 3° warming at the surface (950 mb) and the 5°C cooling at 400 mb.

A remarkable change occurred in the moisture profile. The morning sounding, taken when Monett was in the middle of the comma tail, is nearly saturated from 700 to 350 mb but quite dry in the low troposphere. This particular temperature–moisture profile indicates strong potential *stability* in the 950–700 mb layer. Shortly after 1200 GMT, showers occurred at Monett, moistening the lower layers. Warm temperature advection, indicated by the low-level veering of the winds at both time periods and by Figs. 13a and 14a, continued throughout the day. By 2100 GMT, clouds became broken as the midtropospheric dry surge moved overhead, and the sky was nearly clear by 0000 GMT just before the squall line passed over (Figs. 19, 20). The net effect of all this was to dry out completely the 700–600 mb layer and create potential *instability* in the 950–700 mb layer. For example, the surface θ_e value increased from 296 to 311 K while the 690 mb θ_e decreased from 314 to 301 K. Since surface temperatures in the vicinity where the dry slot convection broke out were near 23°C (Fig. 21), the change in the $\partial\theta_e/\partial p$ gradient during the day in northeast Oklahoma may have been even more dramatic. In terms of the lifted index (LI), the 1200 GMT UMN LI = +12 while the 0000 GMT value decreased to zero. If surface air just ahead of the dryline is used (T = 23°C, T_d = 10°C) and T_{500} = −22° (Fig. 14b), then the LI was −8 when the convection began.

The winds at Monett actually weakened during the day as the low moved closer, except at the surface where they increased to 10 m s^{-1}. The weak midtropospheric winds probably precluded tornado development but the strong low-level directional shear supports the classical self-propagation mechanism

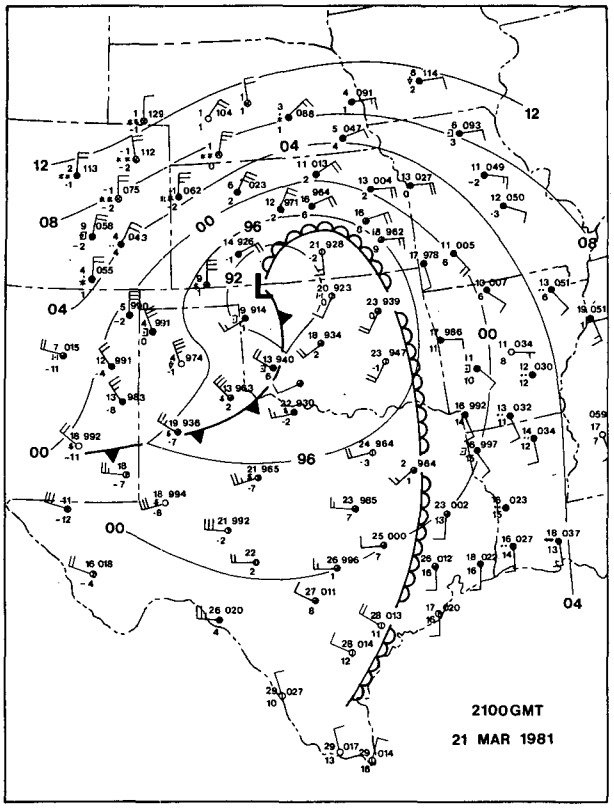

FIG. 21. Surface map over Great Plains states for 2100 GMT 21 March 1981. Solid lines are isobars analyzed every 4 mb; thick lines are fronts; adjacent semicircles indicate a dry line, spaced triangles a cold front. Station data includes temperatures and dew point temperatures in °C, pressure in tenths of mb (with leading 9 or 10 omitted) and winds (full barb: 5 m s^{-1}; half barb: 2.5 m s^{-1}).

proposed for long-lived squall lines (e.g., see Ludlam, 1963; Newton, 1963).

d. Vertical motion

Although results from the composite study and qualitative deductions made from Figs. 13 and 14 suggest that the dry-slot convection was triggered in a region of synoptic-scale rising motion, the gridded data set allows us to verify this contention quantitatively. Three methods of computing vertical motion were utilized: (i) quasi-geostrophic ω-equation; (ii) kinematic technique; and (iii) isentropic flow ω as given by Eq. (2). Only results from the first method will be shown here, although results from the other two will be mentioned briefly.

A 10-level diagnostic quasi-geostrophic numerical model was initialized on a 2.5° latitude–longitude grid with height data (produced by the National Meteorological Center) every 100 mb from 1000–100 mb. Terrain and frictional effects were not included so that $\omega = 0$ at 1000 and 50 mb. In addition to the vorticity and thermal forcing terms in the omega equation, a diabatic term including only the effects of large-scale condensational heating was added. Figure 23 portrays 600 mb ω fields at 1200 GMT 21 March and 0000 GMT 22 March 1981. At 1200 GMT, a large area of upward velocities with a slight comma shape is centered over southwestern Missouri. The atmosphere responds to this with the broad outbreak of clouds and precipitation seen in Figs. 15 and 17. Subsidence is indicated to the west and south of the 500 mb low (Fig. 13), helping to produce the dry air that is subsequently drawn into the storm's circulation, creating the dry tongue.

By 0000 GMT 22 March, the maximum 600 mb upward motion is over northwestern Mississippi, consistent with the satellite and radar views seen in Figs. 19 and 20. It was not expected that quasi-geostrophic omegas would define a separate rising center over the region of dry-slot convection, although this area is undergoing ascent of 2–3 μb s^{-1}. This just reinforces the point that mesoscale forcing (represented by convergence along the surface dry line) can interact with the synoptic scale to generate mesoscale phenomena which are not located in the region of maximum quasi-geostrophic forcing.

It is quite easy to determine the relative contribution of the three forcing terms in the omega equation (Krishnamurti, 1968). Dry dynamics dominated at the 1200 GMT period with differential vorticity advection and thermal advection (not shown) contributing about equally to both rising and sinking motion

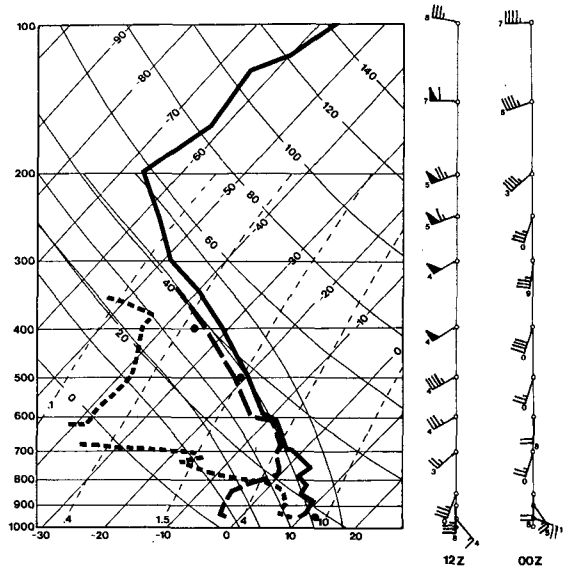

FIG. 22. Skew$T$ – log$p$ diagram for Monett, MO. Thick solid line is 1200 GMT 21 March 1981 temperature profile while long-dashed line is the dew point temperature for the same time. The short-dashed line is the dew point temperature for 0000 GMT 22 March 1981; solid dots at 950, 500 and 400 mb represent temperature values at 0000 GMT. Diagram and wind information is the same as stated in Fig. 10 except that the ten's digit of the wind direction is also plotted.

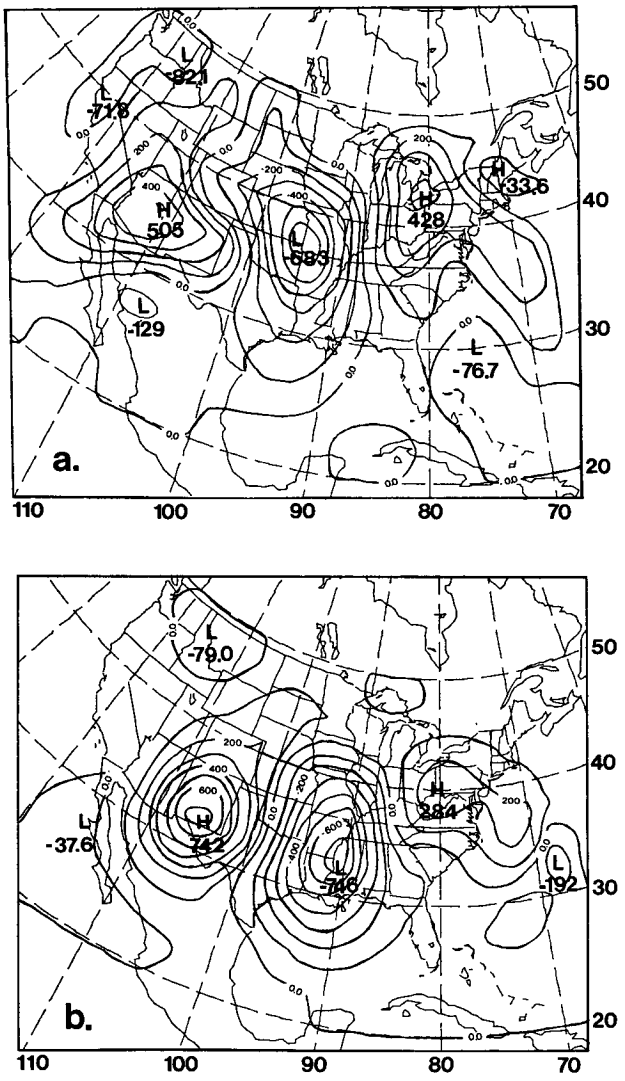

FIG. 23. Quasi-geostrophic ω at 600 mb for (a) 1200 GMT 21 March 1981, (b) 0000 GMT 22 March 1981. Units are in μb s^{-1} $\times$ 100.

maximums. By 0000 GMT 22 March, the thermal advection had weakened and the latent heat of condensation term contributed 3–4 μb s^{-1} to the upward motion center over the lower Mississippi Valley. The upward motion over the region of dry-slot convection was nearly all due to differential cyclonic vorticity advection. Vorticity advection decreasing with height was the primary cause of the strong descent over New Mexico at this time.

Kinematic vertical velocities (not shown) computed using ten levels of wind data spaced 100 mb apart also support the view that weak upward motion does exist over eastern Oklahoma at 0000 GMT with the primary rising center located southeast of that region. The midtropospheric vertical velocities computed on relative-wind, isentropic surfaces for the same period were weaker than the omegas shown in Fig. 23, partly due to the adiabatic assumption, but still averaged 1–2 μb s^{-1} over the region of dry-slot convection.

e. Forecast considerations

Squall lines obviously do not form in the center of every dry intrusion associated with occluding wave cyclones. If a dry tongue similar to those shown in Figs. 1 and 16 is present or is about to form, the following factors should be considered to evaluate whether a new line of convection will form behind the main precipitation areas to the east.

(i) The edge of the midtropospheric clouds on the western boundary of zone C in the comma tail should be moving eastward faster than the associated surface frontal zone or dry line. This creates the possibility of a region of moist boundary-layer air between the thick cloud shield and the surface boundary.

(ii) The aforementioned region should be relatively cloud free (or at least have broken cloud cover) to allow solar radiation to reach the surface. Since dry air is now present aloft over this region, the additional surface heating combines to increase greatly the potential instability of the sounding.

(iii) Since new convection is most likely to begin between 1500 and 2100 LST, factor (ii) suggests that dry slot convection is most likely to begin in a region which clears out aloft by 0900–1500 LST but has not yet experienced passage of the surface boundary.

(iv) Large-scale upward motion should be present in the dry slot. Since, by definition, the dry slot is east and northeast of the midtropospheric vorticity center, differential cyclonic vorticity advection is likely present. Figures 7–9 and 13a, 14a indicate that warm temperature advection is also important in causing rising motion. Since the dry tongue is on the western edge of the large-scale upward motion area, adiabatic cooling has occurred there the longest, further destabilizing the sounding.

(v) The surface boundary can be a cold front, occluded front or dry line (or perhaps no front is analyzed); the important fact is that moisture convergence is present. This rule is included for completeness to remind us that a low-level triggering mechanism is required to release the potential instability. Other traditional criteria for convection and severe weather should also be evaluated. For example, one should especially check for sufficient low-level moisture, and whether the sounding will become unstable enough to support convection.

These factors have been developed from looking at cases over the Great Plains. Over the southeastern United States, where sufficient boundary-layer θ_e values for vigorous convection are nearly always present, the requirement for low-level clearing after the comma tail passes over may not be necessary; the drying and

cooling aloft and presence of a surface triggering mechanism may be sufficient. Also, after a cyclone has occluded and the dry intrusion is drawn well into the circulation and is quite broad at its southern end, more than one line of convection may exist in this expanded dry slot. Careful monitoring of surface boundaries and secondary vorticity advection areas aloft is recommended in order to anticipate each of these.

5. Summary and conclusions

Two separate but related studies have been carried out. The first is a composite study of comma-cloud systems that were observed over the Great Plains during two spring seasons. The second involves the formation of a secondary line of convection within the northeastern part of the dry intrusion, an important feature of the comma system whose mean structure was documented in the first study. In one sense this comma-cloud research represents a composite study of wave cyclones in the stages just before and after the occlusion process. The important point to be made, though, is that the compositing was done with respect to what one sees from the satellite imagery and no reference was made to conventional surface and upper-air maps before the appropriate rawinsonde data were selected.

To obtain a reliable, quantitative description of the comma cloud system, 68 time periods were included. Each comma pattern was divided into ten zones, five in the cloudy region (A–E) and five in the dry tongue (1–5). Rawinsonde data from these zones were composited and interpolated to pressure and isentropic surfaces. Some of the results obtained from the isobaric sectionals are as follows.

(i) The circulation center is located near the eastern side of the comma head at low levels and tilts southwestward with height to the southern edge in the middle troposphere.

(ii) The eastern boundary of the dry tongue (the upper cold front) slopes downstream with height (especially in zone 1), creating a region where low θ_e air overlies moist boundary-layer air. The potential instability thus created may be released near the upper cold front within the warm conveyor belt (convection in zones C, D and E) or near the surface frontal boundary (dry slot convection).

(iii) The data suggest two upper-tropospheric wind speed maxima, one cutting across the southern end of the comma tail and another nearly aligned along the dry slot axis; this implies difluence over the middle sections of the comma tail.

Relative-wind, isentropic analyses constructed for three θ-surfaces indicated that (to the extent that the flow is steady-state and adiabatic) the following situations exist.

(i) The vertical motion is upward in all the cloudy zones except zone A, the comma head; here moist, cool air is advected in from the east as Carlson (1980) found.

(ii) The strongest adiabatic rising motions are in the northern part of the dry tongue, as air with a previous history of descent is drawn into the storm circulation; although warm advection plays an important role in this upward motion, local temperature decreases are observed here as adiabatic cooling dominates.

(iii) The relative wind field portrays a deformation zone in the lower troposphere just to the west of the southern part of the comma tail, consistent with a surface front or dry line at the surface. The wind field also suggests that the western cloud boundary locates the confluent asymptote of the upper cold front.

Composite soundings, θ_e profiles and severe weather indices suggest that zone D is the region most likely to experience severe weather events and this was borne out by NOAA storm data reports (U.S. Dept. of Commerce, 1980–81). At low levels, zone B, north of the warm front, is most stable, while nearly dry adiabatic layers are observed in the southwestern regions of the dry slot, especially at 0000 GMT. Zones 1 and C are somewhat stable in the mean but have large diurnal ranges, as they destabilize significantly during the day. Zones C, D and E reported 80% of the severe weather events; some can occur, however, in the comma head and in zone 1.

The reason for the development of convection in zone 1 was the subject of the second part of this paper. The 21–22 March 1981 comma-cloud system yielded a clear example of the release of potential instability along a surface boundary upstream of the upper cold front (dry-slot convection) that produced a long-lived squall line with heavy rains and small hail. This phenomena is most likely to occur given the sequence of events outlined in Section 4e. The key points are that the advection of drier air aloft must be faster than the movement of the surface boundary and this separation should occur during the day, lasting several hours to allow solar heating of the moist surface air. Although the existence of a dry slot penetrating northward of the comma head is an important ingredient (primarily because of the strong cyclonic-scale rising motion in this region), we have also observed similar occurrences of secondary convective development behind the southern half of the comma tail (zones 2 and 4) if the main cloud band passes over before midafternoon and some moisture remains near the surface.

Because only ten stations at most were involved in each time period and these stations differed in each case, no attempt was made to construct a composite grid. Future work in this area should include gridded

composites so that more detailed kinematic structure, trajectories, budgets and other relevant quantities could be computed. The compositing should also be done with respect to the life cycle of the storm so that a composite time evolution of the three-dimensional structure of the wave cyclone would be available. This would provide an important mean synoptic and dynamic reference state which would complement our present observational knowledge of baroclinic wave development, most of which has been obtained from individual case studies.

Acknowledgments. The data for this project were provided by Mr. Paul Mulder of the Data Support Section of the National Center for Atmospheric Research, which is supported by the National Science Foundation. We would like to thank Drs. Howie Bluestein, Lance Bosart, Toby Carlson, Jeff Kimpel and John McGinley for their helpful comments. Appreciation is expressed to Mohan Ramamurthy, Neal Shores, Terri Cassil and Eric Buchak for assistance with producing and drafting the figures; and to Ginger Knight for typing the manuscript. Support for Jim Millard's graduate studies was provided by the Air Force Institute of Technology. This work was funded in part by NSF Grant ATM-8019430.

APPENDIX

Definition of SWEAT Index

The SWEAT Index I as defined by Miller (1972) is given by

$$I = 12D + 20(TT - 49) + 2f8 + f5 + 125(S + 0.2),$$

where D is the 850 mb dew point temperature in °C, f8 and f5 are 850 mb and 500 mb wind speeds respectively in knots, $S = \sin(\alpha_5 - \alpha_8)$ where α_5 and α_8 are 500 and 850 mb wind directions respectively, and $TT = (T + D)_{850} - 2T_{500}$ is the "total totals" where T is temperature in °C. None of the terms are allowed to be negative; hence if $D < 0$, the first term is set to zero; if $TT < 49$, the second term is set to zero; and the last term is set to zero if any of the following conditions are not met: α_8 between 130 and 250°, α_5 between 210 and 310°, $(\alpha_5 - \alpha_8) > 0$, and both f8, f5 $\geqslant$ 15 knots. The critical value for severe thunderstorms is 300, while $I \geqslant 400$ indicates potential for tornado formation.

According to the nomenclature of Table 1, term one is the "low-level moisture part," term two is the "stability part," terms three and four are the "dynamic part" and term five is the "shear part." Note that the entire index can be computed from just two mandatory-level reports at 850 and 500 mb.

REFERENCES

Anderson, R. K., J. P. Ashman, F. Bittner, G. R. Farr, E. W. Ferguson, V. J. Oliver and A. H. Smith, 1972: Applications of meteorological satellite data in analysis and forecasting. ESSA Tech. Rep. NESC-51, Washington, DC, 260 pp. [NTIS AD-740-017.]

Barr, S., M. B. Lawrence and F. Sanders, 1966: TIROS vortices and large-scale vertical motion. *Mon. Wea. Rev.*, **94,** 675–696.

Boucher, R. J., and R. J. Newcomb, 1962: Synoptic interpretation of TIROS vortex patterns: A preliminary cyclone model. *J. Appl. Meteor.*, **1,** 127–136.

Browning, K. A., 1965: The evolution of tornadic storms. *J. Atmos. Sci.*, **22,** 664–668.

——, 1971: Radar measurements of air motion near fronts. *Weather,* **26,** 320–340.

——, and G. A. Monk, 1982: A simple model for the synoptic analysis of cold fronts. *Quart. J. Roy. Meteor. Soc.*, **108,** 435–452.

Carlson, T. N., 1980: Airflow through midlatitude cyclones and the comma-cloud pattern. *Mon. Wea. Rev.*, **108,** 1498–1509.

——, R. A. Anthes, M. Schwartz, S. G. Benjamin and D. G. Baldwin, 1980: Analysis and prediction of the severe storms environment. *Bull. Amer. Meteor. Soc.*, **61,** 1018–1032.

Cooley, J. R., 1978: Cold air funnel clouds. *Mon. Wea. Rev.*, **106,** 1368–1372.

Crutcher, H. L., and J. M. Meserve, 1970: *Selected Level Heights, Temperatures and Dew Points for the Northern Hemisphere.* NAVAIR 50-1C-52 (revised), Commander, Naval Weather Service Command, Washington, DC, 410 pp.

Green, J. S. A., F. H. Ludlam and J. F. R. McIlveen, 1966: Isentropic relative-flow analysis and the parcel theory. *Quart. J. Roy. Meteor. Soc.*, **92,** 210–219.

Harrold, T. W., 1973: Mechanisms influencing the distribution of precipitation within baroclinic disturbances. *Quart. J. Roy. Meteor. Soc.*, **99,** 232–251.

Kreitzberg, C. W., and H. A. Brown, 1970: Mesoscale weather systems within an occlusion. *J. Appl. Meteor.*, **9,** 417–432.

Krishnamurti, T. N., 1968: A study of a developing wave cyclone. *Mon. Wea. Rev.*, **96,** 208–217.

Leese, J. A., 1962: The role of advection in the formation of vortex cloud patterns. *Tellus,* **14,** 409–421.

Ludlam, F. H., 1963: Severe local storms—A review. *Meteor. Monogr.*, No. 5, Amer. Meteor. Soc., 1–30.

McNulty, R. P., 1978: On upper tropospheric kinematics and severe weather occurrence. *Mon. Wea. Rev.*, **106,** 662–672.

Miller, R. C., 1972: Notes on analysis and severe-storm forecasting procedures of the Air Force Global Weather Central. Air Weather Service Tech. Rep. 200 (Rev.), 190 pp. [NTIS AD-744-042.]

——, and J. A. McGinley, 1978: Using satellite imagery to detect and track comma clouds and the application of the zone technique in forecasting severe storms. 96 pp. [Available from GE Management and Technical Services Company, Beltsville, MD 20705.]

Mullen, S. L., 1979: An investigation of small synoptic-scale cyclones in polar air streams. *Mon. Wea. Rev.*, **108,** 1636–1647.

Newton, C. W., 1963: Dynamics of severe convective storms. *Meteor. Monogr.* No. 5, Amer. Meteor. Soc., 33–58.

Petterssen, S., 1936: A contribution to the theory of frontogenesis. *Geofys. Publ.*, **11,** 1–27.

Schaefer, J. T., 1974: The life cycle of the dryline. *J. Appl. Meteor.*, **13,** 444–449.

U.S. Dept. of Commerce, 1980–81: Storm data. **22–23,** No. 3–6.

Weldon, R. B., 1979: Satellite training course notes, part IV. Cloud patterns and the upper air wind field. 80 pp. [Available from R. B. Weldon, Applications Lab, NESDIS, NOAA, Washington, DC 20233.]

Widger, W. K., Jr., 1964: A synthesis of interpretations of extratropical vortex patterns as seen as TIROS. *Mon. Wea. Rev.*, **92,** 263–282.

Williams, K. T., and W. M. Gray, 1973: Statistical analysis of satellite-observed trade wind cloud clusters in the western North Pacific. *Tellus,* **25,** 313–336.